IEEE Access
Multidisciplinary | Rapid Review | Open Access Journal

Received February 27, 2019, accepted March 12, 2019, date of publication March 15, 2019, date of current version April 2, 2019.

Digital Object Identifier 10.1109/ACCESS.2019.2905367

WLS Localization Using Skipped Filter, Hampel Filter, Bootstrapping and Gaussian Mixture EM in LOS/NLOS Conditions

CHEE-HYUN PARK AND JOON-HYUK CHANG, (Senior Member, IEEE)
Department of Electronic Engineering, Hanyang University, Seoul 133-791, South Korea

Corresponding author: Joon-Hyuk Chang (jchang@hanyang.ac.kr)

This work was supported by the National Research Foundation of Korea (NRF) grant funded by the Korean Government (MSIP) under Grant 2017R1A2A1A17069651.

ABSTRACT We present robust range-based localization algorithms for which range measurements are used to estimate the location parameter. Non-line-of-sight (NLOS) propagation of signal can deteriorate the estimation performance severely in the indoor and crowded urban areas. A study for localization has been intensively performed in the line-of-sight (LOS) conditions, but the work for the positioning in the mixed LOS/NLOS environments is comparatively rare. Thus, we aim at the robust localization in the LOS/NLOS mixture environments. The Hampel and skipped filters-based weighted least squares (WLS) methods are proposed for situations where the variance for inliers is unknown in LOS/NLOS mixture environments. For the unsupervised clustering algorithm, Gaussian mixture expectation maximization-based WLS algorithm is utilized. It is demonstrated that the positioning accuracy of the proposed methods is higher than that of conventional methods through extensive simulation.

INDEX TERMS Localization, robust, Hampel filter, skipped filter, clustering, weighted least squares.

I. INTRODUCTION

Source localization is a technique in which the coordinates of the source are estimated utilizing measurements from each sensor including the time difference of arrival, the time of arrival (TOA), the received signal strength, or the angle of arrival. Localization of the point target is of considerable interest in various fields of research such as telecommunication, radar, sonar and mobile communications. Position estimation problems under line-of-sight (LOS) environments have been intensively studied in previous works [1]–[6]. However, some open problems still exist and a crucial task among location estimation problems is to determine the location of the source in LOS/non-line-of-sight (NLOS) mixed situations [7]–[9]. For example, it may be possible that the LOS between the source and sensors may be obstructed in indoor scenarios.

Generally, we can categorize research regarding location estimation for the LOS/NLOS mixture problem into two kinds: 1) mathematical optimizations [10]–[13], and 2) robust statistics [14]–[19]. We focus on the robust statistics-based localization in this paper.

In general, the variances of inliers for each sensor are assumed to be known in the localization context [1]–[5], [20], but they may be unknown in adverse environments. Consequently, we investigate the robust localization algorithm where the variance of inliers is previously unknown. Meanwhile, it is well known that the Hampel filter and skipped filter have satisfactory estimation performance when outliers exist [21]–[24]. We utilize the Hampel and skipped filters to remove the adverse effects of outliers in the context of LOS/NLOS mixture localization. It should be noted that we combine the concept of the weighting matrix of the weighted least squares (WLS) method with the conventional Hampel and skipped filters to enhance the estimation performance of the Hampel and skipped filters.

Recent works to deal with robust localization in the LOS/NLOS mixture condition are as follows. The bisection localization method has been adopted in the LOS/NLOS mixture condition and the bias is estimated using the mathematical optimization method [25]. A geometrical method which can locate a source based on TOA measurements and floor

The associate editor coordinating the review of this manuscript and approving it for publication was Nan Wu.

plan information is proposed in NLOS indoor environments by converting NLOS problem into LOS problem [26]. The marginalized Monte-Carlo Gaussian smoothing based robust localization has been proposed, where the conditional Gaussian formulation for the skew-t distribution is utilized [27]. An equality constrained Taylor-series robust squares method is developed to suppress the residual NLOS range error [28]. A maximum likelihood estimator (MLE) for robust localization is dealt with, where all the available measurements are used and the probabilities of occurrences of LOS and NLOS propagations are taken into account [29]. Also, machine learning methods have been widely investigated in diverse fields. In [30]–[32], the expectation-maximization (EM) method was adopted. Also, density-based spatial clustering of applications with noise (DBSCAN) algorithm is employed to cluster the multipath components (MPCs) [33] and the grid-based k-NN localization method is devised to estimate the target location in the crowd sourced air traffic communication networks [34]. However, the conventional robust localization algorithms in the LOS/NLOS conditions have not utilized the noise variance information. We improve the performance of the conventional localization method using the weighting matrix (noise variance information) for the samples predicted as the inlier. We summarize our main contributions as follows:

- We develop closed-form robust WLS localization methods that use the weighting matrix comprised of noise variance information by extending the Hampel and skipped filters.
- We propose machine learning based WLS localization method, i.e., the Gaussian mixture EM algorithm. The samples that are determined as inliers are utilized to estimate the variance for the sample mean for the data predicted as inliers.
- The variance of the sample mean for the filtered (classified) data is found algebraically when the variance of inliers is unknown.

To the best of our knowledge, WLS-based approaches combined with the Hampel filter and skipped filter have not yet been investigated in the existing literatures. Furthermore, the Gaussian mixture EM-based WLS algorithm is the first attempt at resolving robust localization problems. Although the Gaussian mixture EM algorithm has been investigated for the localization in [30], the variance information has not been utilized there. Also, note that the proposed methods are the closed-form localization algorithms excluding the Gaussian mixture EM method. The proposed methods require matrix inverse operation whose computational complexity is relatively high. However, the complexity burden can be diminished by updating the inverse matrix intermittently if the environments are slowly varying. Furthermore, the crucial advantage of the proposed Hampel filter-based WLS algorithm and skipped filter-based WLS method is that they are closed-form algorithms. Thus, divergence problem or trapping in the local minima does not occur.

This paper is organized as follows. Section II deals with the LOS/NLOS mixed location estimation problem to be tackled in this work. Section III describes the proposed positioning algorithms using the robust WLS algorithm based on the Hampel filter, skipped filter, unsupervised clustering method and robust bootstrap method. Section IV performs the analysis for the mean square error (MSE) and computational complexity. Section V evaluates the root mean square error (RMSE) performances through simulation results and analysis. Finally, Section VI presents the conclusion.

II. PROBLEM FORMULATION

The aim of the emitter location method using TOA measurements is to accurately predict the coordinates of a point target so that the error criterion, e.g., the MSE or sum of squared error, is minimized. In the context of LOS/NLOS mixed emitter positioning, the measurement equation is determined as

$$r_{i,j} = d_i + n_{i,j} + c_{i,j} = \sqrt{(x - x_i)^2 + (y - y_i)^2} + n_{i,j} + c_{i,j}, \tag{1}$$

where $n_{i,j}$ is distributed by $(1-\epsilon)N(0, \sigma_1^2)+\epsilon N(\mu_2, \sigma_2^2)$, $i = 1, 2, \ldots, M$, $j = 1, 2, \ldots, P$ with M and P denoting the number of sensors and samples in the ith sensor, respectively [30], [35]–[37]. Also, $c_{i,j}$ is the clock synchronization error defined as $\hat{t}_{i,j} - d_i$ ($\hat{t}_{i,j}$ is the estimated range using the clock synchronization algorithm for the ith sensor and jth time instance ([38], [39])) and d_i is the true range between the emitter and ith receiver. The measurement error $n_{i,j}$ is the random process that follows a two-mode Gaussian mixture distribution in which the LOS noise component is distributed as $N(0, \sigma_1^2)$ and the NLOS noise follows $N(\mu_2, \sigma_2^2)$ ($N(\mu, \sigma^2)$ denotes a Gaussian probability density function (PDF) with mean μ and variance σ^2). The LOS noise has a probability of $1-\epsilon$ and the LOS/NLOS noise has a probability of ϵ. Unlike previous research for the LOS/NLOS mixture localization, the mean and variance of the inlier and outlier distribution are unavailable. Here, ϵ ($0 \le \epsilon \le 1$) is a measure of contamination, which is usually lower than 0.1 [35]–[37], $[x \;\; y]^T$ is the unknown emitter coordinates and $[x_i \;\; y_i]^T$ is the known coordinates of the ith receiver. Also, $r_{i,j}$ is the range measurement between the point target and the ith receiver at the jth time instance. Squaring (1) and rearranging yield the following equation:

$$x_i x + y_i y - 0.5R + m_{i,j} = 0.5({x_i}^2 + {y_i}^2 - r_{i,j}^2), \quad i = 1, 2, \ldots, M, \quad j = 1, 2, \ldots, P \tag{2}$$

where $R = x^2 + y^2, m_{i,j} = -d_i n_{i,j} - n_{i,j}c_{i,j} - d_i c_{i,j} - \frac{1}{2}n_{i,j}^2 - \frac{1}{2}c_{i,j}^2$. Representing (2) in a matrix form, we obtain the following

$$\mathbf{A}\mathbf{x} + \mathbf{m}_j = \mathbf{b}_j, \quad j = 1, \cdots, P \tag{3}$$

where $\mathbf{m}_j = [m_{1,j}, \cdots, m_{M,j}]^T$, $\mathbf{x} = [x\ y\ R\ ]^T$,

$$\mathbf{A} = \begin{pmatrix} x_1 & y_1 & -0.5 \\ \vdots & \vdots & \vdots \\ x_M & y_M & -0.5 \end{pmatrix}, \quad \text{and}$$

$$\mathbf{b}_j = [b_{1,j} \cdots b_{M,j}]^T = \frac{1}{2}\begin{pmatrix} x_1^2 + y_1^2 - r_{1,j}^2 \\ \vdots \\ x_M^2 + y_M^2 - r_{M,j}^2 \end{pmatrix}.$$

Throughout this paper, a vector is presented with a lowercase boldface letter, a matrix with an uppercase boldface letter and the operator $[\cdot]^T$ denotes a vector/matrix transpose.

III. PROPOSED LOCALIZATION METHOD

In general, the variance for inliers is assumed to be known in the context of localization. However, the noise statistics of inliers may be unknown in certain adverse environments. Thus, we develop the robust WLS localization algorithms that do not require the variance of inliers as *a priori*. Below, we explain in detail the proposed Hampel filter-based WLS, skipped filter-based WLS, robust bootstrap-based WLS, and Gaussian-mixture EM-based WLS methods. For more details of the WLS algorithm, refer to [40].

A. THE HAMPEL FILTER-BASED WLS ALGORITHM

In this subsection, the Hampel filter-based WLS localization algorithm is in detail described. Specifically, Hampel filter's response is given by:

$$y_{i,j} = \begin{cases} b_{i,j}, & |b_{i,j} - m_i| < tD_i; \\ m_i, & |b_{i,j} - m_i| > tD_i \end{cases} \tag{4}$$

where m_i is the median value from the moving data window and D_i is the median absolute deviation (MAD) scale estimate of the ith sensor, defined as: $D_i = 1.4826 \times \text{median}|b_{i,1:P} - m_i|$. The parameter t is empirically selected by the experiment and this parameter is determined by searching for the minimum point in the RMSE plot. As the other method, 2.5 or 3 was suggested in [41] and [42], respectively. The threshold, 3, is the reasonable and natural value by the 3-σ edit rule. The filtered data, $y_{i,1:P}$, are averaged using the sample mean, i.e., $b_i^{h,f} = \frac{\sum_{p=1}^{P} y_{i,p}}{P}$. Then, the variance of the statistic $b_i^{h,f}$ is found via algebraic methods as follows:

$$\text{Var}[b_i^{h,f}] = \begin{cases} \dfrac{S_{i1}}{P^2}, & \text{if } i \in \mathbf{\Lambda}; \\ \dfrac{S_{i2} + \dfrac{\pi}{2} \times \dfrac{S_{i2}}{Q_i^2} \times R_i}{P^2}, & \text{if } i \in \mathbf{\Lambda}^c \end{cases} \tag{5}$$

where $S_{i1} = \sum_p (y_{i,p} - me_{i1})^2$, p's are the sample indices which are associated with the ith LOS sensor, $S_{i2} = \sum_{q_i} (y_{i,q_i} - me_{i2})^2$, q_i's are the sample indices for the samples which are predicted as inliers in the ith LOS/NLOS mixture sensor, Q_i is the number of samples predicted as inliers in the ith LOS/NLOS mixture sensor, R_i is the number of samples determined as outliers in the ith LOS/NLOS mixture sensor, $P = (Q_i + R_i)$ is the total number of samples in the ith sensor, $me_{i1} = \frac{1}{P}\sum_{p=1}^{P} y_{i,p}$ and $me_{i2} = \frac{1}{Q_i}\sum_{q_i=1}^{Q_i} y_{i,q_i}$. Also, $\mathbf{\Lambda}$ is the LOS set in which the elements are indices of sensors which are predicted as the LOS sensors and $\mathbf{\Lambda}^c$ is the LOS/NLOS mixture set where the components are indices of sensors predicted as LOS/NLOS mixture sensors. Namely, all measurements are inliers in the LOS sensor and at least one outlier exists in the LOS/NLOS mixture sensor. In the numerator of the second equation of (5), the constant $\frac{\pi}{2}$ is introduced because the variance of the median is asymptotically larger than the variance of the sample mean by $\frac{\pi}{2}$ times [14]. $\text{Var}[b_i^{h,f} \in \mathbf{\Lambda}]$ and $\text{Var}[b_i^{h,f} \in \mathbf{\Lambda}^c]$ were derived in the following manner:

$$\begin{aligned} &\text{Var}[b_i^{h,f} \in \mathbf{\Lambda}] \\ &= \frac{\text{Var}[\text{one inlier of the } i\text{th sensor } (i \in \mathbf{\Lambda})] \times \text{IN}}{P^2} \\ &= \frac{\frac{S_{i1}}{P} \times P}{P^2}, \end{aligned} \tag{6}$$

$$\begin{aligned} &\text{Var}[b_i^{h,f} \in \mathbf{\Lambda}^c] \\ &= \frac{\text{Var}[\text{one inlier of the } i\text{th sensor } (i \in \mathbf{\Lambda}^c)] \times \text{IN}}{P^2} \\ &\quad + \frac{\text{Var}[\text{median for } y_{i,1:P} (i \in \mathbf{\Lambda}^c)] \times \text{OUT}}{P^2} \\ &= \frac{\frac{S_{i2}}{Q_i} \times Q_i + \frac{\pi}{2} \times \frac{S_{i2}}{Q_i^2} \times R_i}{P^2} \end{aligned} \tag{7}$$

where IN and OUT denote the number of inliers and number of outliers, respectively. Then, the transformed measurement equation for the WLS estimator using the Hampel-filter is determined as follows:

$$\mathbf{A}\mathbf{x} + \boldsymbol{\varepsilon} = \mathbf{b}^{h,f} \tag{8}$$

where $\boldsymbol{\varepsilon} = [\varepsilon_1, \cdots, \varepsilon_M]^T$, $\mathbf{b}^{h,f} = [b_1^{h,f} \cdots b_M^{h,f}]^T$ and $\boldsymbol{\varepsilon}$ is the noise components of $\mathbf{b}^{h,f}$. Finally, the WLS estimate based on the Hampel filter is determined in the following:

$$\hat{\mathbf{x}}_{h,f} = (\mathbf{A}^T \mathbf{W}^{h,f} \mathbf{A})^{-1} \mathbf{A}^T \mathbf{W}^{h,f} \mathbf{b}^{h,f} \tag{9}$$

where $\mathbf{W}^{h,f} = \mathbf{C}_{\mathbf{b}^{h,f}}^{-1} = (\text{diag}[\text{Var}\{b_1^{h,f}\} \cdots \text{Var}\{b_M^{h,f}\}])^{-1}$. Furthermore, the accuracy of the first-step estimate can be improved using the well-known second-step approach [2], [3] and is represented as given below:

$$\hat{\mathbf{x}}_{h,s} = (\mathbf{H}^T \mathbf{C}_{\hat{\mathbf{h}}}^{-1} \mathbf{H})^{-1} \mathbf{H}^T \mathbf{C}_{\hat{\mathbf{h}}}^{-1} \hat{\mathbf{h}} \tag{10}$$

where

$$\hat{\mathbf{h}} = \left[[\hat{\mathbf{x}}_{h,f}]_1^2 \ [\hat{\mathbf{x}}_{h,f}]_2^2 \ [\hat{\mathbf{x}}_{h,f}]_3 \right]^T, \quad \text{and} \tag{11}$$

$$\mathbf{H} = \begin{pmatrix} 1 & 0 \\ 0 & 1 \\ 1 & 1 \end{pmatrix}, \tag{12}$$

$$\mathbf{C}_{\hat{\mathbf{h}}} = \text{diag}[2x\ 2y\ 1](\mathbf{A}^T \mathbf{C}_{\mathbf{b}^{h,f}}^{-1} \mathbf{A})^{-1} \text{diag}[2x\ 2y\ 1] \tag{13}$$

$$\simeq \mathbf{X}(\mathbf{A}^T \mathbf{C}_{\mathbf{b}^{h,f}}^{-1} \mathbf{A})^{-1} \mathbf{X}^T, \tag{14}$$

$[\mathbf{a}]_r$ is the rth component of vector $\boldsymbol{a}$ and $\mathbf{X} = \text{diag}[2[\hat{\mathbf{x}}_{h,f}]_1 \; 2[\hat{\mathbf{x}}_{h,f}]_2 \; 1]$. The final second-step WLS emitter position estimate is given as follows:

$$\hat{\mathbf{x}}_f = \left[\text{sgn}([\hat{\mathbf{x}}_{h,f}]_1)\sqrt{[\hat{\mathbf{x}}_{h,s}]_1} \quad \text{sgn}([\hat{\mathbf{x}}_{h,f}]_2)\sqrt{[\hat{\mathbf{x}}_{h,s}]_2}\right]^T \tag{15}$$

where $\text{sgn}(\cdot)$ denotes the sign function.

B. THE SKIPPED FILTER-BASED WLS ALGORITHM

In the Hampel filter of the previous section, when the absolute value of the difference between the sample and median is larger than the threshold, the sample median is substituted for the corresponding sample. In contrast, in the skipped filter, when the sample is predicted as an outlier, the corresponding sample is removed from the sample set of the sensor. The filtered data, y_{i,q_i}, are averaged using the sample mean, i.e., $b_i^{s,f} = \sum_p \frac{y_{i,p}}{P}$ in the LOS sensor or $b_i^{s,f} = \sum_{q_i} \frac{y_{i,q_i}}{Q_i}$ in the LOS/NLOS mixture sensor. Then, the variance of the statistic $b_i^{s,f}$ is found algebraically in the same manner as the Hampel filter-based WLS method:

$$\text{Var}[b_i^{s,f}] = \begin{cases} \dfrac{S_{i1}}{P^2}, & \text{if } i \in \boldsymbol{\Lambda}; \\ \dfrac{S_{i2}}{Q_i^2}, & \text{if } i \in \boldsymbol{\Lambda}^c. \end{cases} \tag{16}$$

The WLS estimate based on the skipped filter is found as given below:

$$\hat{\mathbf{x}}_{s,f} = (\mathbf{A}^T\mathbf{W}^{s,f}\mathbf{A})^{-1}\mathbf{A}^T\mathbf{W}^{s,f}\mathbf{b}^{s,f} \tag{17}$$

where $\mathbf{b}^{s,f} = [b_1^{s,f} \cdots b_M^{s,f}]^T$ and $\mathbf{W}^{s,f} = \mathbf{C}_{\mathbf{b}^{s,f}}^{-1} = (\text{diag}[\text{Var}\{b_1^{s,f}\} \cdots \text{Var}\{b_M^{s,f}\}])^{-1}$. Furthermore, the second-step solution is obtained in the same manner as in Section 3.1.

C. ROBUST BOOTSTRAP-BASED WLS ALGORITHM

The samples are taken randomly with replacement like the bootstrap method, but the difference from the existing bootstrap method is that the samples whose absolute difference from the median is smaller than the threshold (to be determined through the empirical experiment) are only taken in the variance calculation. On the contrary, in the conventional bootstrap method, samples are selected randomly with replacement in the calculation of variance, independent of the absolute difference between the median and the corresponding sample. Thus, the existing bootstrap method would evidently include the outlier in the evaluation of the variance and fail to estimate the variance of inliers in the situation that outliers exist. The inverse of the estimated variance is determined as the weight in the robust bootstrap-based WLS algorithm and the variance estimation procedure is summarized in Algorithm 1. Also, the WLS estimate based on the robust bootstrap algorithm is represented as follows:

$$\hat{\mathbf{x}}_{s,b} = (\mathbf{A}^T\mathbf{W}^{s,b}\mathbf{A})^{-1}\mathbf{A}^T\mathbf{W}^{s,b}\mathbf{b}^{s,b} \tag{18}$$

where $\mathbf{W}^{s,b} = (\text{diag}[\text{Var}\{b_1^{s,b}\} \cdots \text{Var}\{b_M^{s,b}\}])^{-1}$ and $\mathbf{b}^{s,b}$ is identical to $\mathbf{b}^{s,f}$ defined in (17). The second-step solution can be obtained in the same manner as Section 3.1. The disadvantage of the robust bootstrap method is that the computational complexity is higher than those of the Hampel filter, skipped filter and unsupervised clustering-based WLS algorithms.

Algorithm 1 Robust Bootstrap-Based Variance Estimation Procedure

Suppose $\mathbf{b}_i^* = (b_{i,1}^*, b_{i,2}^*, \cdots, b_{i,P}^*)$ are samples which are selected randomly with replacement from given data $\mathbf{b}_i = (b_{i,1}, b_{i,2}, \cdots, b_{i,P})$.

1. Resample the bootstrap samples $\mathbf{b}_i^{*1}, \mathbf{b}_i^{*2}, \cdots \mathbf{b}_i^{*C}$ independently. If $|\mathbf{b}_i^{*c}(p) - m_i^c| > tD$, do a resampling until $|\mathbf{b}_i^{*c}(p) - m_i^c| \le tD$ (m_i^c is the median of $\mathbf{b}_i^{*c}$, t and D are the same with those in [22] and $\mathbf{b}_i^{*c}(p)$ denotes the pth element of $\mathbf{b}_i^{*c}$).
2. Calculate the sample variance in each $\mathbf{b}_i^{*c}$ as $\text{Var}(\mathbf{b}_i^{*c}) = \frac{\sum_{p=1}^{P}(\mathbf{b}_i^{*c}(p) - \bar{\mathbf{b}}_i^{*c})^2}{P}$ ($\bar{\mathbf{b}}_i^{*c}$ is the sample mean for $\mathbf{b}_i^{*c}$).
3. Determine $\text{Var}(b_i^{s,b}) = \frac{\sum_{c=1}^{C}\text{Var}(\mathbf{b}_i^{*c})}{C}$, where $b_i^{s,b}$ is the ith element of $\mathbf{b}^{s,b}$.
4. Repeat 1-3 for all sensors.

D. THE GAUSSIAN MIXTURE EM-BASED WLS ALGORITHM

Gaussian mixture EM-based outlier detection has been investigated in [30]. However, the existing robust algorithm does not employ the weights for sensors. In the proposed Gaussian mixture EM-based WLS method, we devise a way to use the weight (inverse of variance). The number of clusters of the Gaussian mixture is two because two-mode Gaussian mixture distribution has been widely used in the existing literatures [30]. The samples are labeled as inliers or outliers using the Gaussian mixture EM algorithm. The samples that are determined as inliers are utilized to estimate the variance of the sample mean for the data determined as inliers and the samples that are predicted as outliers are removed. As a consequence, the variance of the sample mean for the data predicted as inliers is calculated in the following:

$$\text{Var}[b_i^{g,f}] = \begin{cases} \dfrac{S_{i1}}{P^2}, & \text{if } i \in \boldsymbol{\Lambda}; \\ \dfrac{S_{i2}}{Q_i^2}, & \text{if } i \in \boldsymbol{\Lambda}^c. \end{cases} \tag{19}$$

Finally, the first-step and second-step WLS estimates based on the Gaussian mixture EM algorithm are derived in the same manner as that described in the Section 3.1.

IV. PERFORMANCE ANALYSIS

A. MSE PERFORMANCE ANALYSIS

In this section, we analyze the MSEs of the proposed methods. The MSE is the sum of the squared bias and variance. The RMSE can be obtained by taking the square root of the MSE. The estimation error $\Delta\widehat{\mathbf{x}}_f$ is represented as

$$\Delta\widehat{\mathbf{x}}_f \tag{20}$$

$$= \mathbf{D}_2^{-1}\Delta\widehat{\mathbf{x}}_{h,s} \tag{21}$$

TABLE 1. Comparison of the computational complexity.

Algorithm	Computational complexty
Two-step WLS (WLS_1)	$O(N^2M + NM^2 + N^3)$
Weighted Skipped Filter	$O(N^2M + NM^2 + N^3)$
Weighted Hampel Filter	$O(N^2M + NM^2 + N^3)$
Gaussian Mixture EM	$O(IN^3 + N^2M + NM^2 + N^3)$
Bisection	$2 \times O(IM)$

$$= \mathbf{D}_2^{-1}(\mathbf{H}^T\mathbf{C}_{\widehat{\mathbf{h}}}^{-1}\mathbf{H})^{-1}\mathbf{H}^T\mathbf{C}_{\widehat{\mathbf{h}}}^{-1}(\widehat{\mathbf{h}} - \mathbf{H}\mathbf{x}_{h,s}) \quad (22)$$

$$= \mathbf{D}_2^{-1}(\mathbf{H}^T\mathbf{C}_{\widehat{\mathbf{h}}}^{-1}\mathbf{H})^{-1}\mathbf{H}^T\mathbf{C}_{\widehat{\mathbf{h}}}^{-1}\mathbf{D}_1(\widehat{\mathbf{x}}_{h,f} - \mathbf{x}_{h,f}) \quad (23)$$

$$= \mathbf{G}(\mathbf{A}^T\mathbf{C}_{\mathbf{b}^{h,f}}^{-1}\mathbf{A})^{-1}\mathbf{A}^T\mathbf{C}_{\mathbf{b}^{h,f}}^{-1}(\mathbf{b}^{h,f} - \mathbf{A}\mathbf{x}_{h,f}) \quad (24)$$

where $\mathbf{D}_1 = \mathrm{diag}[2x \;\; 2y \;\; 1]$, $\mathbf{D}_2 = 2\mathrm{diag}[x \;\; y]$, $\mathbf{G} = \mathbf{D}_2^{-1}(\mathbf{H}^T\mathbf{C}_{\widehat{\mathbf{h}}}^{-1}\mathbf{H})^{-1}\mathbf{H}^T\mathbf{C}_{\widehat{\mathbf{h}}}^{-1}\mathbf{D}_1$ and $\mathbf{x}_{h,f}, \mathbf{x}_{h,s}$ are the true values for $\widehat{\mathbf{x}}_{h,f}$, $\widehat{\mathbf{x}}_{h,s}$. Then, the error covariance matrix of $\widehat{\mathbf{x}}_f$ is represented as follows:

$$\mathrm{cov}[\Delta\widehat{\mathbf{x}}_f] = \mathbf{G}(\mathbf{A}^T\mathbf{C}_{\mathbf{b}^{h,f}}^{-1}\mathbf{A})^{-1}\mathbf{G}^T. \quad (25)$$

Because $E[\widehat{\mathbf{h}}] \simeq \mathbf{h}$ in the sufficiently small noise condition, the bias for the second step estimate of the Hampel filter-based WLS estimate is approximately the zero vector. Thus, the bias of the final solution for the Hampel filter-based WLS algorithm is the zero vector. Then, $\mathrm{MSE}(\hat{\mathbf{x}}_f) \simeq \mathrm{tr}[\mathrm{cov}(\hat{\mathbf{x}}_f)]$, where $\mathrm{tr}(\cdot)$ denotes the trace operator. Furthermore, the MSEs of the skipped filter-based WLS method and the Hampel filter-based WLS estimator are nearly the same because each diagonal component of $\mathbf{C}_{\mathbf{b}^{s,f}}$ is similar with that of $\mathbf{C}_{\mathbf{b}^{h,f}}$. Evidently, the diagonal components of the covariance matrices are the same when $i \in \mathbf{\Lambda}$. When $i \in \mathbf{\Lambda}^c$, using the property that $P \gg R_i$ the following property is satisfied

$$\frac{S_{i2}}{Q_i^2} \simeq \frac{S_{i2} + \frac{\pi}{2}\frac{S_{i2}}{Q_i}R_i}{P^2}, \quad i \in \mathbf{\Lambda}^c. \quad (26)$$

Therefore, the MSEs of the skipped filter-based WLS and Hampel filter-based WLS methods are nearly the same under the condition of $P \gg R_i$.

B. COMPUTATIONAL COMPLEXITY ANALYSIS

Table 1 shows the computational complexity of the existing robust algorithms and proposed algorithms, where M is the number of sensors, N is the number of parameters and I is the iteration number. The computational complexity was dependent on the matrix inverse and multiplication operations because their computational load is higher than that of other operations. The computational complexity of the Gaussian mixture EM was higher than that of the weighted skipped and Hampel filters due to the discerning operations of the inliers and outliers. Also, it should be noticed that the RMSE performance of the Gaussian mixture EM is severely degraded when the standard deviation of LOS noise is large (see Fig. 4). Therefore, it can be concluded that weighted skipped and weighted Hampel filters have competitive advantages in both respects of the localization accuracy and computational complexity compared to the other algorithms. Although, the proposed algorithms require the matrix inverse operation, inverse matrix may be updated intermittently in the slowly varying environments. Then, the computational complexity can be much diminished.

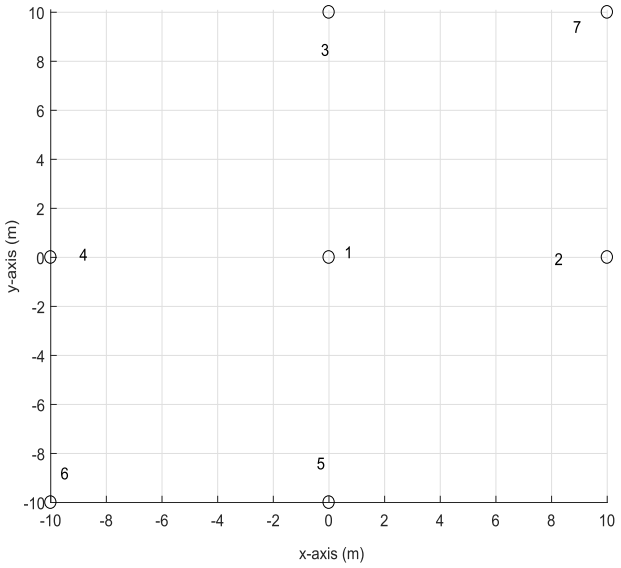

FIGURE 1. Deployment of sensors.

V. SIMULATION RESULTS

We compared the performance of the proposed LOS/NLOS mixed emitter positioning methods with that of the robust WLS method [20] and bisection estimator [25] in this section. The simulation setting is provided in Table 2.

The RMSE is defined as follows:

$$\mathrm{RMSE} = \sqrt{\frac{\sum_{i=1}^{10}\sum_{k=1}^{200}[(\widehat{x}^k(i) - x(i))^2 + (\widehat{y}^k(i) - y(i))^2]}{10 \times 200}} \quad (27)$$

where $\widehat{x}^k(i)$, $\widehat{y}^k(i)$ is the estimated location of the point target in the ith position set and kth iteration and $x(i)$ and $y(i)$ denote the ith true coordinates of the emitter. Fig. 1 shows the arrangement of the receivers. Although we used the fixed sensor deployment in this simulation, the RMSE performance varies according to the geometry of sensors. This observation can be justified by the concept of the geometric dilution of precision (GDOP) (the localization accuracy is better as the GDOP is lower). The localization accuracy with respect to the standard deviation of the NLOS error is displayed in Fig. 2. In Fig. 2(a), the contamination ratio (ϵ) was 20%, the sample size was 20, the bias of the NLOS error (μ_2) was 4 m, the standard deviation of the LOS noise (σ_1) was 0.1 m, t was 3, receivers 5, 6 and 7 were the LOS/NLOS mixture sensors and the remaining receivers were LOS sensors. It is evident that RMSEs of the proposed robust WLS methods were lower than those of the other existing methods. The

TABLE 2. Simulation settings.

Source location	a single source located within a 20×20 m^2 region
Number of simulated sources	10
Number of Monte-Carlo simulation	200
LOS noise variance of each sensor	assumed to be identical
Number of receivers	7
Directivity of source	omni-direction

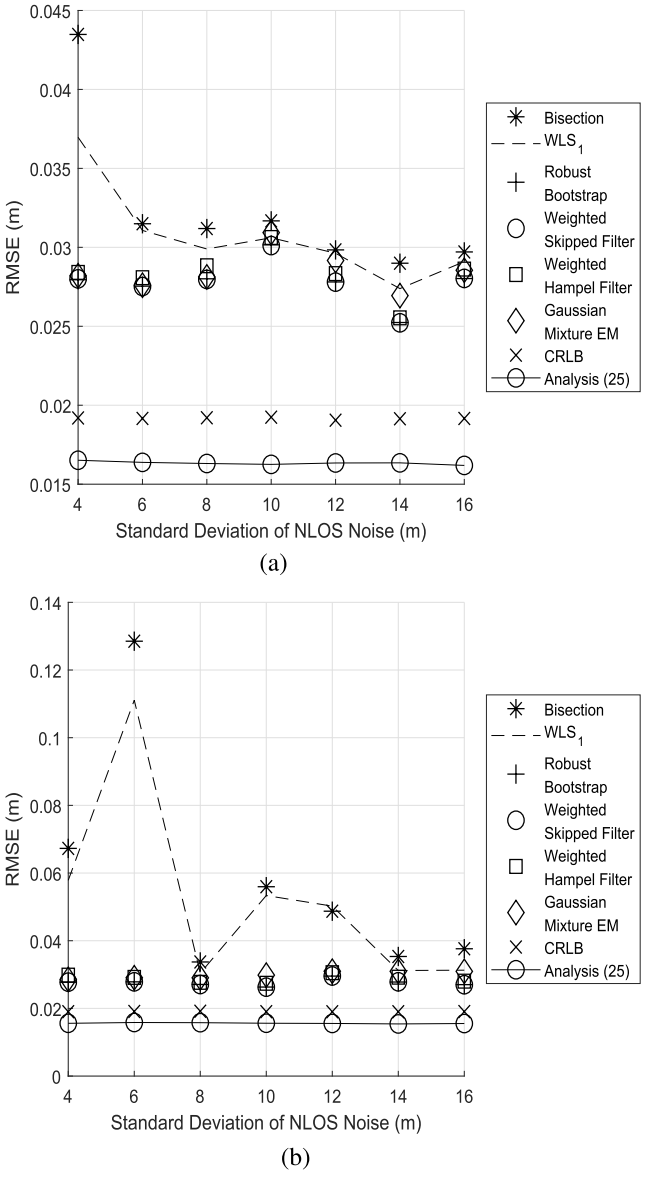

FIGURE 2. Comparison of RMSEs of the proposed estimators with that of the existing methods when the sensor 5, 6 and 7 are the LOS/NLOS mixture sensors and the remaining sensors are the LOS sensors. (a) contamination ratio (ϵ): 20 %, the bias of NLOS noise (μ_2): 4 m, standard deviation of LOS noise (σ_1): 0.1 m. (b) ϵ: 30 %, σ_1: 0.1 m, μ_2: 4 m.

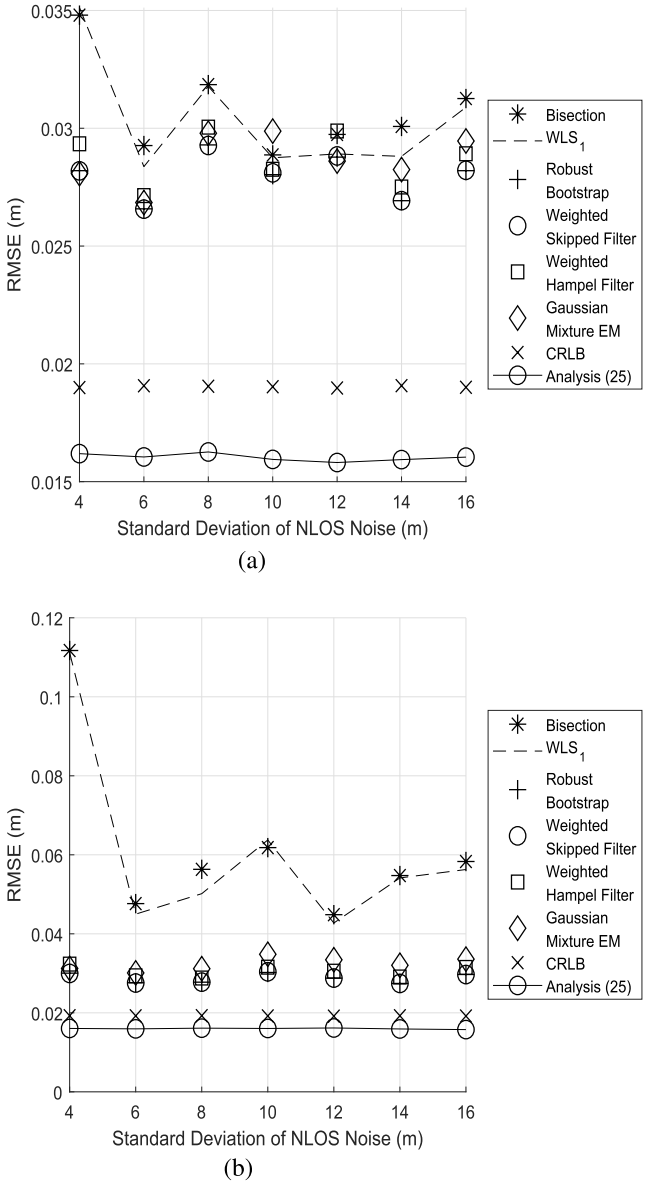

FIGURE 3. Comparison of RMSEs of the proposed estimators with that of the existing methods when the sensor 4, 5, 6 and 7 are the LOS/NLOS mixture sensors and the remaining sensors are the LOS sensors. (a) contamination ratio (ϵ): 20 %, the bias of NLOS noise (μ_2): 4 m, standard deviation of LOS noise (σ_1): 0.1 m. (b) ϵ: 30 %, σ_1: 0.1 m, μ_2: 4 m.

RMSEs of the proposed algorithms were about 2.8 cm and the RMSEs of the bisection and existing WLS methods were about 3.0 cm in Fig. 2(a). The proposed methods outperformed the bisection and existing robust WLS methods by about 0.2 cm. The RMSEs of the proposed weighted skipped filter and weighted Hampel filter were nearly the same. The CRLB was 1.9 cm and it was calculated using the numerical approximation [30]. The RMSE by an analysis using (25) was

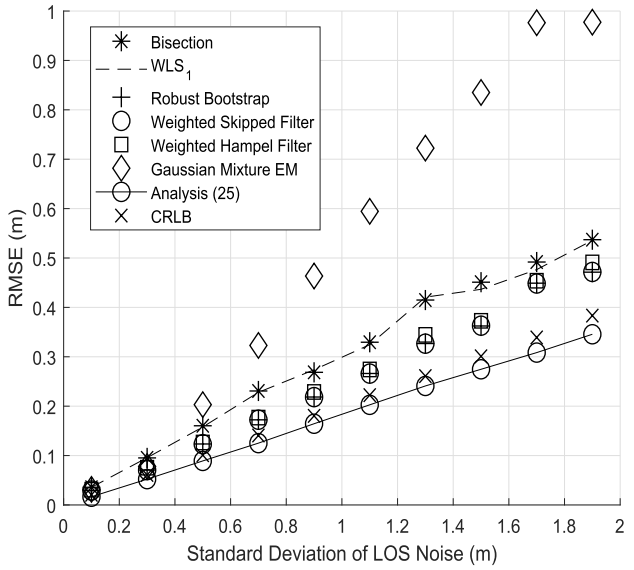

FIGURE 4. RMSEs of the localization algorithms as a function of standard deviation of LOS noise (bias of NLOS noise (μ_2): 4 m, contamination ratio: 30%, standard deviation of NLOS noise (σ_2): 10 m).

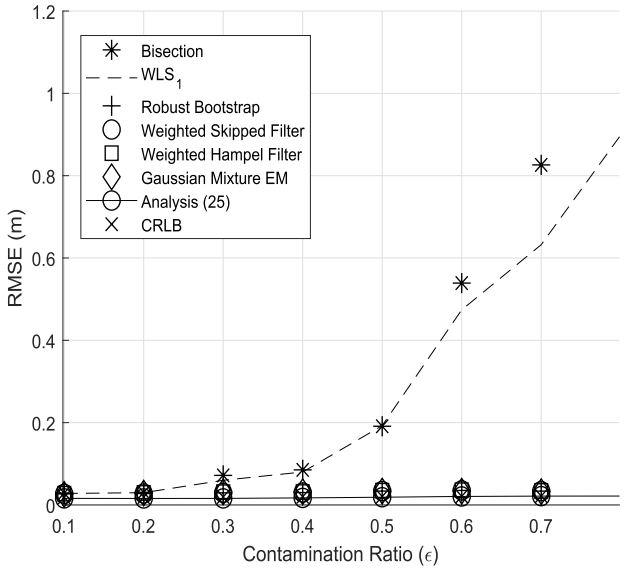

FIGURE 5. RMSEs of the localization algorithms as a function of contamination ratio (bias of NLOS noise (μ_2): 4 m, contamination ratio: 30%, standard deviation of LOS noise (σ_1): 0.1 m, standard deviation of NLOS noise (σ_2): 10 m).

1.7 cm. The RMSEs of the proposed methods were larger than the CRLB by about 0.9 cm. In Fig. 2(b), the contamination ratio was 30%, while the remaining environments were identical with those in Fig. 2(a). The RMSEs of the proposed methods were about 3.0 cm and the RMSEs of the bisection and existing WLS methods were 4.0 cm. In Fig. 2(b), the proposed methods outperformed the bisection and existing robust WLS methods by about 1.0 cm. The CRLB was 2.0 cm and the RMSEs of the proposed methods were larger than the CRLB by 1.0 cm. The error variance by an analysis using (25) was 1.9 cm.

Fig. 3 postulates the same environment as that in Fig. 2, except that receivers 4, 5, 6 and 7 are the LOS/NLOS mixture receivers. The RMSEs of the proposed methods were about 2.7 cm and those of the bisection and existing WLS methods were about 3 cm in Fig. 3(a). Namely, the RMSEs of the proposed algorithms were lower than the existing algorithms by 0.3 cm. The CRLB was 1.9 cm and the RMSEs of the proposed methods were larger than the CRLB by about 0.8 cm. The error variance by an analysis using (25) was 1.7 cm. In Fig. 3(b), the RMSEs of the proposed algorithms were about 3.0 cm and those of the bisection and existing WLS methods were about 6.0 cm. That is, the RMSEs of the proposed algorithms were lower than those of the existing algorithms by 3.0 cm. The CRLB was 2.0 cm and the RMSEs of the proposed algorithms were larger than the CRLB by 1.0 cm. The error variance by an analysis using (25) was 1.9 cm.

Indeed, Fig. 4 shows the RMSEs vs. the standard deviation of inliers. In Fig. 4, sensors 1, 2, 3 and 4 were assumed to be the LOS sensors, sensors 5, 6 and 7 were the LOS/NLOS mixture sensors and the contamination ratio was 30%. The RMSEs of the proposed methods were lower than those of the other methods in Fig. 4. The performances of all robust methods got worse as the standard deviation of LOS error was increased. The RMSEs of the proposed methods approximated the CRLB in the small LOS noise regimes, but moderately degraded than the CRLB in the high LOS noise conditions.

Next, Fig. 5 illustrates the RMSEs vs. the contamination ratio. Again, the proposed robust WLS-based methods outperformed the other methods, as shown in Fig. 5. When the contamination ratio became larger than 50%, the RMSEs of the existing robust methods were significantly increased. However, those of the proposed methods were nearly constant. This observation is due to the usage of the weights that are larger as the sample variance is lower. Thus, the adverse effects of outliers can be attenuated using the proposed robust WLS algorithm although the contamination ratio is larger than 50%.

Fig. 6 shows the RMSEs vs. the bias. The RMSEs of all methods were nearly constant as the bias varied and the proposed methods outperformed the other existing algorithms. Namely, the localization performances of the proposed WLS-based algorithms are not affected by the bias because the bias is filtered by the skipped and Hampel filters.

Fig. 7 illustrates the RMSEs vs. sample size. As the sample size increased, the RMSEs of all methods decreased and proposed methods outperformed the existing algorithms. The RMSEs of the proposed methods were moderately larger than the CRLB in small sample condition, but the difference from the CRLB was decreased as the sample size increased. In particular, the RMSEs of the proposed algorithms were much superior to that of existing algorithms when the sample size was small.

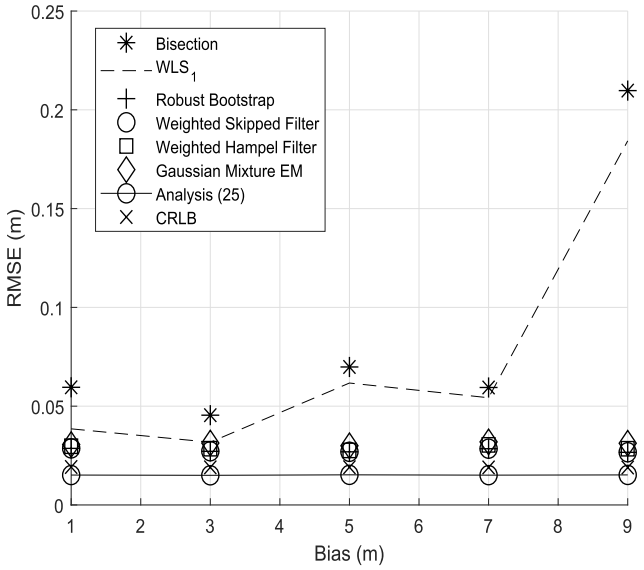

FIGURE 6. RMSEs of the localization algorithms as a function of bias (contamination ratio: 30%, standard deviation of LOS noise (σ_1): 0.1 m, standard deviation of NLOS noise (σ_2): 10m).

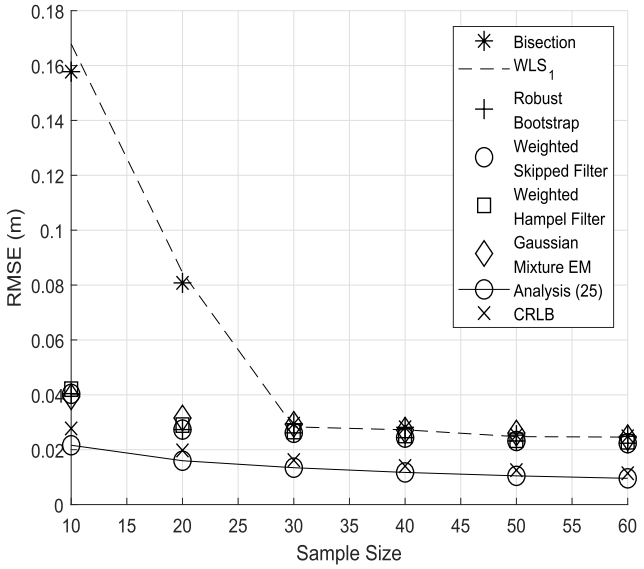

FIGURE 7. RMSEs of the localization algorithms as a function of sample size (bias of NLOS noise (μ_2): 4 m, contamination ratio: 30%, standard deviation of LOS noise (σ_1): 0.1 m, standard deviation of NLOS noise (σ_2): 10m).

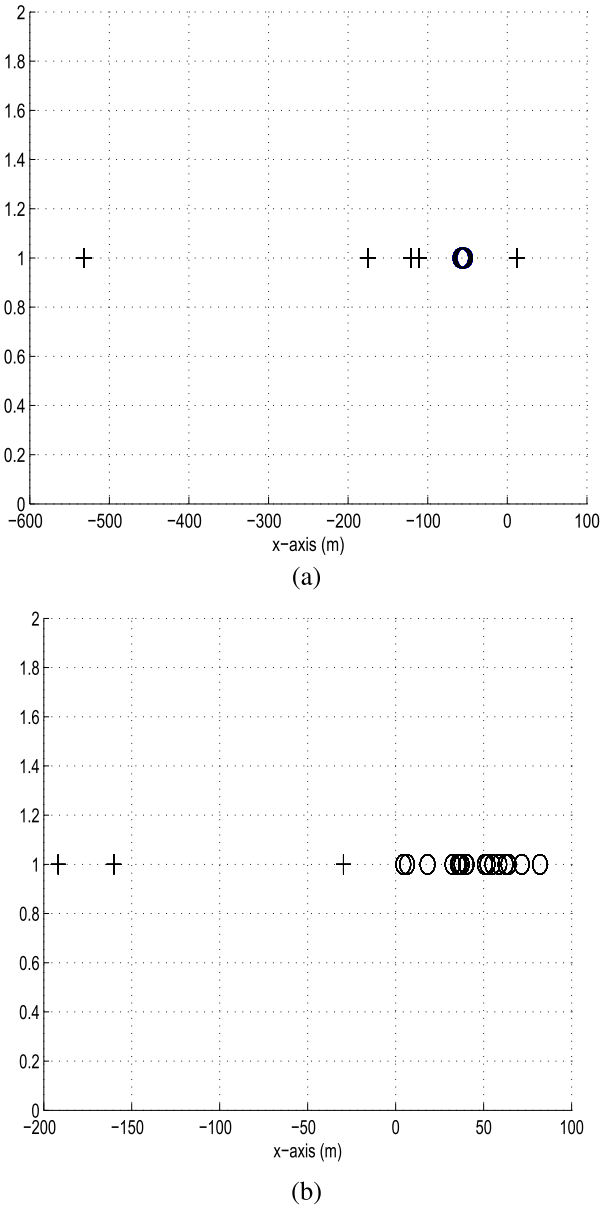

FIGURE 8. Clustering of inliers (o) and outliers (+) set using the Gaussian mixture EM. (a) bias of NLOS noise (μ_2): 4 m, contamination ratio: 30%, standard deviation of LOS noise (σ_1): 0.1 m, standard deviation of NLOS noise (σ_2): 10m. (b) bias of NLOS noise (μ_2): 4 m, contamination ratio: 30%, standard deviation of LOS noise (σ_1): 0.25 m, standard deviation of NLOS noise (σ_2): 10 m.

The clustering result when using the Gaussian mixture EM method is exhibited in Fig. 8. The circles denote the inliers and crosses are the outliers. Fig. 8(a) represents the clustering result in the low inlier noise condition ($\sigma_1 = 0.1$ m) and Fig. 8(b) is that in the high inlier noise condition ($\sigma_1 = 0.25$ m). The clustering was accurately performed in Fig. 8(a) when the inlier noise level was low, but some outliers were wrongly classified as inliers when the inlier noise level was high in Fig. 8(b). Thus, as can be seen from Fig. 4, the RMSE performance of the Gaussian mixture EM algorithm deteriorated as the level of inlier noise increased compared to the other algorithms. Therefore, it is desirable to utilize the Hampel filter, skipped filter and robust bootstrap-based WLS algorithms rather than the unsupervised clustering based WLS method when the noise level of inliers is high.

Finally, Fig. 9 shows the diagonal components of $\mathbf{C}_{\mathbf{b}^{s,f}}$ when the sensors 1, 2, 3 and 4 are LOS sensors, the 5, 6 and 7 sensors are LOS/NLOS mixture sensors and $\epsilon = 0.8$. The variances of LOS sensors were significantly lower than those of the LOS/NLOS mixture sensors. This observation is caused because the median value is not robust to outliers any more when $\epsilon \geq 0.5$. Therefore, the localization performance

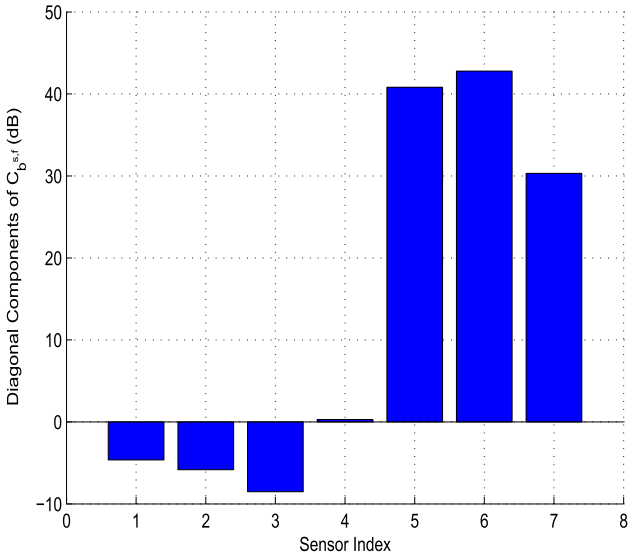

FIGURE 9. Diagonal components of $C_{bs,f}$ when sensors 1, 2, 3 and 4 are LOS sensors, sensors 5, 6 and 7 are LOS/NLOS mixture sensors and $\epsilon = 0.8$.

of the proposed methods was not drastically deteriorated even when $\epsilon \geq 0.5$ unlike the existing robust WLS algorithm because LOS sensors exist.

VI. CONCLUSIONS

The robust range-based WLS localization methods were developed utilizing the Hampel filter, skipped filter, robust bootstrap and unsupervised clustering algorithms. The proposed methods employed the weighting matrix determined from the proposed Hampel filter, skipped filter, unsupervised clustering and robust bootstrap-based methods. The RMSE performances of the proposed WLS-based methods were superior to the existing algorithms. The unsupervised clustering based WLS algorithm was effective in discerning the outliers and inliers in the high SNR condition of inliers, but deteriorated as the noise level of inliers increased. Furthermore, theoretical performance analysis was provided for the proposed methods.

REFERENCES

[1] D. J. Torrieri, "Statistical theory of passive location systems," *IEEE Trans. Aerosp. Electron. Syst.*, vol. AES-20, no. 2, pp. 183–198, Mar. 1984.
[2] Y. T. Chan and K. C. Ho, "A simple and efficient estimator for hyperbolic location," *IEEE Trans. Signal Process.*, vol. 42, no. 8, pp. 1905–1915, Aug. 1994.
[3] H. C. So and L. Lin, "Linear least squares approach for accurate received signal strength based source localization," *IEEE Trans. Signal Process.*, vol. 59, no. 8, pp. 4035–4040, Aug. 2011.
[4] C.-H. Park and J.-H. Chang, "Closed-form localization for distributed MIMO radar systems using time delay measurements," *IEEE Trans. Wireless Commun.*, vol. 15, no. 2, pp. 1480–1490, Feb. 2016.
[5] C. -H. Park, and J.-H. Chang, "Shrinkage estimation-based source localization with minimum mean squared error criterion and minimum bias criterion," *Digit. Signal Process.*, vol. 29, pp. 100–106, Jun. 2014.
[6] J. A. Belloch, A. Gonzalez, A. M. Vidal, and M. Cobos, "On the performance of multi-GPU-based expert systems for acoustic localization involving massive microphone arrays," *Expert Syst. Appl.*, vol. 42, no. 13, pp. 5607–5620, Aug. 2015.
[7] I. Guvenc and C.-C Chong, "A survey on TOA based wireless localization and NLOS mitigation techniques," *IEEE Commun. Surveys Tuts.*, vol. 11, no. 3, pp. 107–124, 3rd Quart., 2009.
[8] A. M. Zoubir, V. Koivunen, Y. Chakhchoukh, and M. Muma, "Robust estimation in signal processing: A tutorial-style treatment of fundamental concepts," *IEEE Signal Process. Mag.*, vol. 29, no. 4, pp. 61–80, Jul. 2012.
[9] N. Kbayer and M. Sahmoudi, "Performances analysis of GNSS NLOS bias correction in urban environment using a three-dimensional city model and GNSS simulator," *IEEE Trans. Aerosp. Electron. Syst.*, vol. 54, no. 4, pp. 1799–1814, Aug. 2018.
[10] S. Zhang, S. Gao, and G. Wang, "Robust NLOS error mitigation method for TOA-based localization via second-order cone relaxation," *IEEE Commun. Lett.*, vol. 19, no. 12, pp. 2210–2213, Dec. 2015.
[11] G. Wang, H. Chen, Y. Li, and N. Ansari, "NLOS error mitigation for TOA-based localization via convex relaxation," *IEEE Trans. Wireless Commun.*, vol. 13, no. 8, pp. 4119–4131, Aug. 2014.
[12] R. M. Vaghefi, J. Schloemann, and R. M. Buehrer, "NLOS mitigation in TOA-based localization using semidefinite programming," in *Proc. 10th Workshop Positioning, Navigat. Commun. (WPNC)*, Dresden, Germany, Mar. 2013, pp. 1–6.
[13] R. M. Vaghefi and R. M. Buehrer, "Cooperative localization in NLOS environments using semidefinite programming," *IEEE Commun. Lett.*, vol. 19, no. 8, pp. 1382–1385, Aug. 2015.
[14] P. J. Rousseeuw and A. M. Leroy, *Robust Regression and Outlier Detection*, Hoboken, NJ, USA: Wiley, 1987.
[15] Z. Li, W. Trappe, Y. Zhang, and B. Nath, "Robust statistical methods for securing wireless localization in sensor networks," in *Proc. 4th Int. Symp. Inf. Process. Sensor Netw.*, Boise, ID, USA, Apr. 2005, pp. 91–98.
[16] R. Casas, A. Marco, J. J. Guerrero, and J. Falcó, "Robust estimator for non-line-of-sight error mitigation in indoor localization," *EURASIP J. Adv. Signal Process.*, vol. 2006, Dec. 2006, Art. no. 43429.
[17] C.-H. Park, S. Lee, and J.-H. Chang, "Robust closed-form time-of-arrival source localization based on α-trimmed mean and Hodges–Lehmann estimator under NLOS environments," *Signal Process.*, vol. 111, pp. 113–123, Jun. 2015.
[18] X.-W. Chang and Y. Guo, "Huber's M-estimation in relative GPS positioning: Computational aspects," *J. Geodesy*, vol. 79, nos. 6–7, pp. 351–362, Aug. 2005.
[19] J. L. Hodges and E. L. Lehmann, "Estimates of location based on rank tests," *Ann. Math. Stat.*, vol. 34, no. 2, pp. 598–611, 1963.
[20] C.-H. Park and J.-H. Chang, "Robust time-of-arrival source localization employing error covariance of sample mean and sample median in line-of-sight/non-line-of-sight mixture environments," *Eurasip J. Adv. Signal Process.*, vol. 2016, pp. 1–11, Dec. 2016.
[21] R. Wilkox, *Introduction to Robust Estimation and Hypothesis Testing*, 3rd ed. San Diego, CA, USA: Academic, 2012.
[22] R. K. Pearson, Y. Neuvo, J. Astola, and M. Gabbouj, "Generalized hampel filters," *EURASIP J. Adv. Signal Process.*, vol. 2016, pp. 1–18, Dec. 2016.
[23] F. R. Hampel, "The breakdown points of the mean combined with some rejection rules," *Technometrics*, vol. 27, no. 2, pp. 95–107, 1985.
[24] L. Davies and U. Gather, "The identification of multiple outliers," *J. Amer. Stat. Assoc.*, vol. 88, no. 423, pp. 782–792, 1993.
[25] S. Tomic and M. Beko, "A bisection-based approach for exact target localization in NLOS environments," *Signal Process.*, vol. 143, pp. 328–335, Feb. 2018.
[26] D. Liu, Y. Wang, P. He, Y. Zhai, and H. Wang, "TOA localization for multipath and NLOS environment with virtual stations," *EURASIP J. Wireless Commun. Netw.*, vol. 2017, no. 104, pp. 1–7, Dec. 2009.
[27] J. V. Valls and P. Closas, "NLOS mitigation in indoor localization by marginalized Monte Carlo Gaussian smoothing," *Eurasip J. Adv. Signal Process.*, vol. 2017, p. 62, Dec. 2017.
[28] K. Yu, K. Wen, Y. Li, S. Zhang, and K. Zhang, "A novel NLOS mitigation algorithm for UWB localization in harsh indoor environments," *IEEE Trans. Veh. Technol.*, vol. 68, no. 1, pp. 686–699, Jan. 2019.
[29] X. Shi, G. Mao, Z. Yang, and J. Chen, "MLE-based localization and performance analysis in probabilistic LOS/NLOS environment," *Neurocomputing*, vol. 270, pp. 101–109, Nov. 2017.
[30] F. Yin, C. Fritsche, F. Gustafsson, and A. M. Zoubir, "EM- and JMAP-ML based joint estimation algorithms for robust wireless geolocation in mixed LOS/NLOS environments," *IEEE Trans. Signal Process.*, vol. 62, no. 1, pp. 168–182, Jan. 2014.

[31] W. Yuan, N. Wu, B. Etzlinger, Y. Li, C. Yan, and L. Hanzo, "Expectation–maximization-based passive localization relying on asynchronous receivers: Centralized versus distributed implementations," *IEEE Trans. Commun.*, vol. 67, no. 1, pp. 668–681, Jan. 2019.
[32] Z. Sjanic, M. A. Skoglund, and F. Gustafsson, "EM-SLAM with inertial/visual applications," *IEEE Trans. Aerosp. Electron. Syst.*, vol. 53, no. 1, pp. 273–285, Feb. 2017.
[33] R. He *et al.*, "A kernel-power-density-based algorithm for channel multipath components clustering," *IEEE Trans. Wireless Commun.*, vol. 16, no. 11, pp. 7138–7151, Nov. 2017.
[34] M. Strohmeier, V. Lenders, and I. Martinovic, "A k-NN-based localization approach for crowdsourced air traffic communication networks," *IEEE Trans. Aerosp. Electron. Syst.*, vol. 54, no. 3, pp. 1519–1529, Jun. 2018.
[35] Y. Feng, C. Fritsche, F. Gustafsson, and A. M. Zoubir, "TOA-based robust wireless geolocation and Cramér-Rao lower bound analysis in harsh LOS/NLOS environments," *IEEE Trans. Signal Process.*, vol. 61, no. 9, pp. 2243–2255, May 2013.
[36] F. Gustafsson and F. Gunnarsson, "Mobile positioning using wireless networks: Possibilities and fundamental limitations based on available wireless network measurements," *IEEE Signal Process. Mag.*, Vol. 22, no. 4, pp. 41–53, Jul. 2005.
[37] U. Hammes, E. Wolsztynski, and A. M. Zoubir, "Robust tracking and geolocation for wireless networks in NLOS environments," *IEEE J. Sel. Top. Signal Process.*, vol. 3, no. 5, pp. 889–901, Oct. 2009.
[38] Y. Xiong, N. Wu, Y. Shen, and M. Z. Win, "Cooperative network synchronization: Asymptotic analysis," *IEEE Trans. Signal Process.*, vol. 66, no. 3, pp. 757–772, Feb. 2018.
[39] S. P. Chepuri, R. T. Rajan, G. Leus, and A.-J. van der Veen, "Joint clock synchronization and ranging: Asymmetrical time-stamping and passive listening," *IEEE Signal Process. Lett.*, vol. 20, no. 1, pp. 51–54, Jan. 2013.
[40] S. M. Kay, *Fundamentals of Statistical Signal Processing: Estimation Theory*, vol. 1, Englewood Cliffs, NJ, USA: Prentice-Hall, 1993.
[41] C. Leys, C. Ley, O. Klein, P. Bernard, and L. Licata, "Detecting outliers: Do not use standard deviation around the mean, use absolute deviation around the median," *J. Experim. Social Psychol.*, vol. 49, no. 4, pp. 764–766, Jul. 2013.
[42] J. Miller, "Reaction time analysis with outlier exclusion: Bias varies with sample size," *Quart. J. Exp. Psychol. Sect. A*, vol. 43, no. 4, pp. 907–912, 1991. 10.1080/14640749108400962.

Authors' photographs and biographies not available at the time of publication.